

Polarizable Water Networks in Ligand–Metalloprotein Recognition. Impact on the Relative Complexation Energies of Zn-Dependent Phosphomannose Isomerase with D-Mannose 6-Phosphate Surrogates

Nohad Gresh,^{*†} Benoit de Courcy,^{†,‡,§} Jean-Philip Piquemal,^{‡,§} Johanna Foret,^{||,⊥} Stéphanie Courtiol-Legourd,^{||,⊥} and Laurent Salmon^{||,⊥}

[†]Laboratoire de Chimie et Biochimie Pharmacologiques et Toxicologiques, UMR8601 CNRS, Univ Paris Descartes, UFR Biomédicale, Faculté de Médecine de Paris, F-75006, Paris, France

[‡]Laboratoire de Chimie Théorique, UPMC Univ Paris 06, UMR7616, F-75252, Paris, France

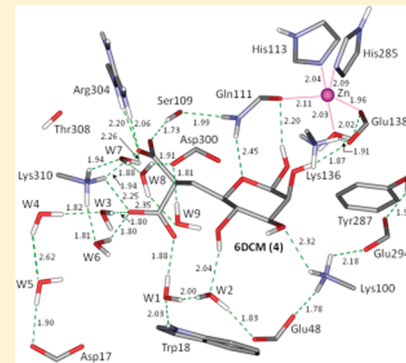
[§]Laboratoire de Chimie Théorique, CNRS, UMR7616, F-75252, Paris, France

^{||}Laboratoire de Chimie Bioorganique et Bioinorganique, Univ Paris-Sud, ICMMO, UMR8182, F-91405, Orsay, France

[⊥]Laboratoire de Chimie Bioorganique et Bioinorganique, CNRS, ICMMO, UMR8182, F-91405, Orsay, France

Supporting Information

ABSTRACT: Using polarizable molecular mechanics, a recent study [de Courcy et al. *J. Am. Chem. Soc.*, 2010, 132, 3312] has compared the relative energy balances of five competing inhibitors of the FAK kinase. It showed that the inclusion of structural water molecules was indispensable for an ordering consistent with the experimental one. This approach is now extended to compare the binding affinities of four active site ligands to the Type I Zn-metallocenzyme phosphomannose isomerase (PMI) from *Candida albicans*. The first three ones are the PMI substrate β -D-mannopyranose 6-phosphate (β -M6P) and two isomers, α -D-mannopyranose 6-phosphate (α -M6P) and β -D-glucopyranose 6-phosphate (β -G6P). They have a dianionic 6-phosphate substituent and differ by the relative configuration of the two carbon atoms C1 and C2 of the pyranose ring. The fourth ligand, namely 6-deoxy-6-dicarboxymethyl- β -D-mannopyranose (β -6DCM), is a substrate analogue that has the β -M6P phosphate replaced by the nonhydrolyzable phosphate surrogate malonate. In the energy-minimized structures of all four complexes, one of the ligand hydroxyl groups binds Zn(II) through a water molecule, and the dianionic moiety binds simultaneously to Arg304 and Lys310 at the entrance of the cavity. Comparative energy-balances were performed in which solvation of the complexes and desolvation of PMI and of the ligands are computed using the Langlet–Claverie continuum reaction field procedure. They resulted into a more favorable balance in favor of β -M6P than α -M6P and β -G6P, consistent with the experimental results that show β -M6P to act as a PMI substrate, while α -M6P and β -G6P are inactive or at best weak inhibitors. However, these energy balances indicated the malonate ligand β -6DCM to have a much lesser favorable relative complexation energy than the substrate β -M6P, while it has an experimental 10-fold higher affinity than it on Type I PMI from *Saccharomyces cerevisiae*. The energy calculations were validated by comparison with parallel ab initio quantum chemistry on model binding sites extracted from the energy-minimized PMI-inhibitor complexes. We sought to improve the models upon including explicit water molecules solvating the dianionic moieties in their ionic bonds with the Arg304 and Lys310 side-chains. Energy-minimization resulted in the formation of three networks of structured waters. The first water of each network binds to one of the three accessible anionic oxygens. The networks extend to PMI residues (Asp17, Glu48, Asp300) remote from the ligand binding site. The final comparative energy balances also took into account ligand desolvation in a box of 64 waters. They now resulted into a large preference in favor of β -6DCM over β -M6P. The means to further augment the present model upon including entropy effects and sampling were discussed. Nevertheless a clear-cut conclusion emerging from this as well as our previous study on FAK kinase is that both polarization and charge-transfer contributions are critical elements of the energy balances.



reactions, guanosine diphosphate-D-mannose and, subsequently, dolichol phosphate-D-mannose. Both precursors are essential in the biosynthesis of mannosylated structures such as glycoproteins, nucleotide sugars, lipopolysaccharides, fungi cell wall components, and bacterial exopolysaccharides.^{4–7} Consequently, PMIs are considered as potential therapeutic targets for the treatment of several diseases of microbial and parasitic origins, such as illness of immuno-suppressed individuals, opportunistic infections in patients with cystic fibrosis, and leishmaniasis.^{8–13} However, there are no presently known PMI inhibitors of use in therapy.

Type I PMIs have been shown to have very similar characteristics with a high level of sequence identity in the region of the active site,^{14,15} which suggests that conclusions that may be drawn from *Candida albicans* PMI can most likely be applied to other Type I PMI, and notably to *Saccharomyces cerevisiae* PMI. Indeed, sequence alignment of the two enzymes show that active site residues are 100% conserved (Figure 2). One of our laboratories has designed a nanomolar inhibitor of PMI, 5-phospho-D-arabinonohydroxamic acid (SPAHA).¹⁶ Its complex with Type I PMI from *C. albicans* (CaPMI) in several competing structures has been modeled by the SIBFA (Sum of Interactions Between Fragment Ab initio computed) polarizable molecular mechanics (PMM) procedure.^{17,18} In a theoretical study of Type I PMI reaction mechanism, the complex of CaPMI with its substrate β -M6P was also recently modeled by the SIBFA

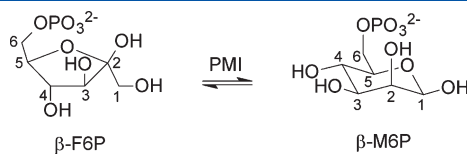


Figure 1. Reversible interconversion of β -D-fructofuranose (β -F6P) to β -D-mannopyranose 6-phosphate (β -M6P) catalyzed by phosphomannose isomerase.

procedure.^{18,19} In order to further define the substrate binding properties of CaPMI, we report here the SIBFA modeling study of two isomers of β -M6P (**1**), its anomer α -D-mannopyranose 6-phosphate (α -M6P, **2**) and its epimer on carbon 2 β -D-glucopyranose 6-phosphate (β -G6P, **3**, Figure 3). Of these, only β -M6P (**1**) acted as a PMI ligand, α -M6P (**2**) and β -G6P (**3**) being reported as inactive or at best weak inhibitors of Type I PMI from *S. cerevisiae* (ScPMI).^{1,20} We have subsequently sought to increase both the resistance of β -M6P analogues against enzymatic degradation and their cellular permeability. This was done by replacing the dianionic 6-phosphate moiety of β -M6P (**1**) by a malonate one, yielding 6-deoxy-6-dicarboxymethyl- β -D-mannopyranose (β -6DCM, **4**) as depicted in Figure 3. Such a replacement was found to result into a 10-fold enhancement of the binding potency on Type I ScPMI.¹⁹

These experimental results are the incentive of the present work. We evaluate the extent to which PMM energy balances can rank the four ligands in conformity with the experimental results. In the first part of this study, we perform balances that encompass, on the one hand, the energy-minimized value of the PMI-ligand complex plus the solvation energy of the complex, calculated with a multipolar continuum reaction field method,²¹ and on the other hand the energy-minimized values of uncomplexed

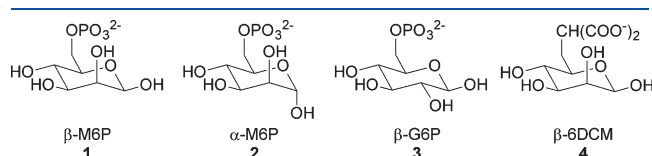


Figure 3. PMI active site ligands evaluated through SIBFA computations in this study: β -D-mannopyranose 6-phosphate (β -M6P, **1**), α -D-mannopyranose 6-phosphate (α -M6P, **2**), β -D-glucopyranose 6-phosphate (β -G6P, **3**), 6-deoxy-6-dicarboxymethyl- β -D-mannopyranose (β -6DCM, **4**).

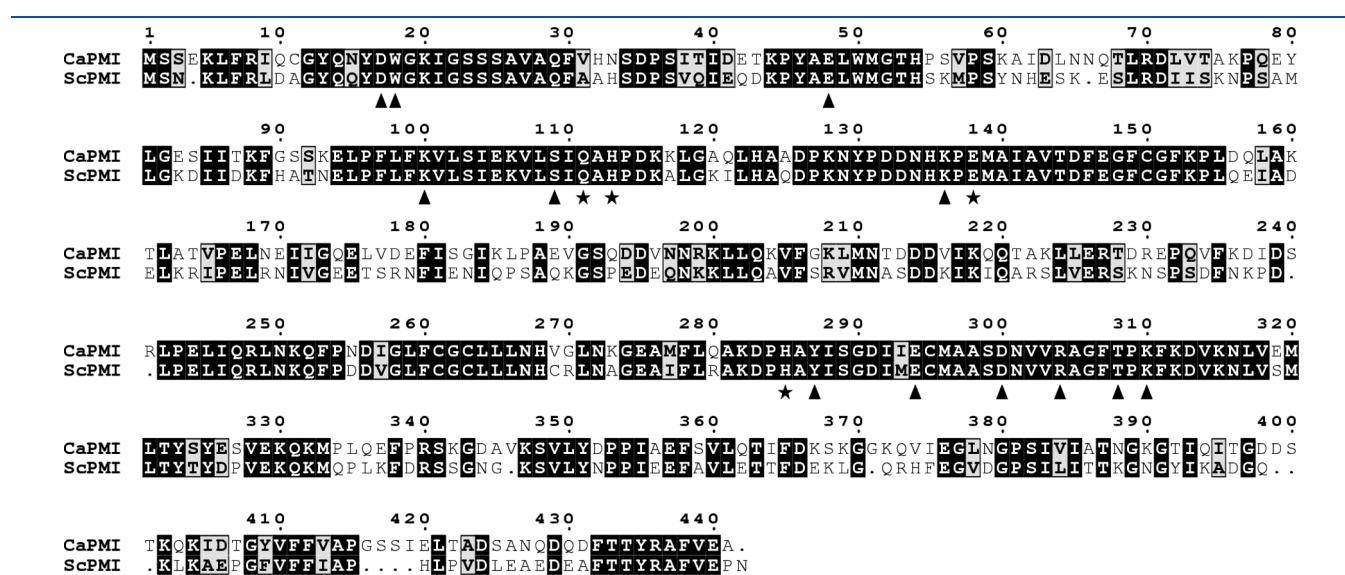


Figure 2. Amino acid sequence alignment of PMIs from *C. albicans* (CaPMI) and *S. cerevisiae* (ScPMI). The sequence numbering corresponds to CaPMI. The alignment length is 442 aa with residues that are conserved in all sequences shown as white characters with a black background (277 residues, 62.67%). Residues that are similar in both sequences are shown as black characters with a gray background (39 residues, 8.82%). The zinc ligands are labeled with an asterisk at the bottom of the alignment. The other residues shown in the energy-minimized structures of the CaPMI active site are labeled with a triangle. This alignment was achieved with CLUSTALW⁵⁹ on NPS@ server⁶⁰ and was illustrated with ESPript (similarity calculations parameters used: type = % of equivalent residues; global score = 0.8).⁶¹

protein and uncomplexed ligand minimized in the presence of this continuum reaction field. In a recent study that bore on the binding of five anionic inhibitors to the FAK kinase,²² it was found essential to augment such a model by including explicitly structural, highly polarized water molecules in the binding site. These waters were seen to complement and/or mediate the interactions taking place between the ligand and the protein. We have investigated their possible impact in the PMI-substrate/inhibitor complexes as well.

■ PROCEDURE

PMM Calculations. We have resorted to the SIBFA procedure.^{23–25} ΔE is a sum of five separate contributions, each of which as a counterpart from ab initio quantum chemistry: $\Delta E = E_{\text{MTP}}^* + E_{\text{rep}} + E_{\text{pol}} + E_{\text{ct}} + E_{\text{disp}}$, which denote the penetration-augmented multipolar contribution, the short-range, polarization, charge-transfer, and dispersion contributions, respectively. Details of the procedure are given in refs 26–28. A model of Type I PMI from *C. albicans* was assembled from the constitutive fragments of the original protein as indicated in ref 17. Energy-minimizations (E-M) were done with the polyvalent “Merlin” software.²⁹ The inhibitors were initially docked with the help of computer graphics in order to maximally overlap with the SPAH inhibitor, whose preferential mode of binding was previously determined by E-M.¹⁷ Such an overlap was recently illustrated in a paper proposing a reaction mechanism for type I phosphomannose isomerases.¹⁸ After initial E-Ms, none of the hydroxyl groups was able to bind Zn(II) at distances closer than 2.5 Å. Therefore we have retained in the model the structural, Zn-bound water, mediating Zn-hydroxyl binding. The inhibitors were fully relaxed in internal coordinates. The PMI backbone was held rigid. E-M was performed on the side-chains of the following residues: Asp17, Trp18, Glu48, Lys100, Ser109, Gln111, His113, Lys136, Glu138, His285, Tyr287, Glu294, Asp300, Arg304, and Lys310. As in our previous work,^{17,22} the computation of ΔG_{solv} was done with the Langlet–Claverie (LC) continuum reaction field procedure in which the electrostatic contribution was computed with the same ab initio distributed multipoles²¹ as for the computation of ΔE .

Quantum Chemistry (QC) Calculations. The QC calculations done to validate the PMM results were done at both Hartree–Fock (HF) and density functional theory/Perdew–Burke–Ernzerhof (DFT/PBE)^{30,31} levels. They used the CEP 4-31G(2d),³² the 6-311G**, and the cc-pVTZ(-f)³³ basis sets. The calculations of the solvation energies were done with the Polarizable Continuum Model (PCM) procedure developed by Tomasi and co-workers.³⁴ The calculations used the Gaussian 09 software.³⁵

Acid–Base Titration. Each titration was done in 0.01 M water solution of ligands. β -M6P (**1**) and β -6DCM (**4**) were titrated by NaOH (0.02 M) with the pH values ranging from 1.75 to 12 and from 2.09 to 12, respectively. Titration curves can be found in the Supporting Information Figure S1.

pK_a Determinations. The number of exchanged protons (Δx)³⁶ was determined using the formula $\Delta x = -(n_{\text{base}} - n_{\text{OH}^-})/n_{\text{reagent}}$, where n_{base} (NaOH) is the number of moles of base added, n_{OH^-} is the number of moles of OH[−] in solution recalculated from the pH value, and n_{reagent} is the mole number of the molecule that is titrated. $\Delta x < 0$ indicates the number of protons that has been removed from the reagent. The variation of Δx as a function of [H⁺] was fitted with the formula shown

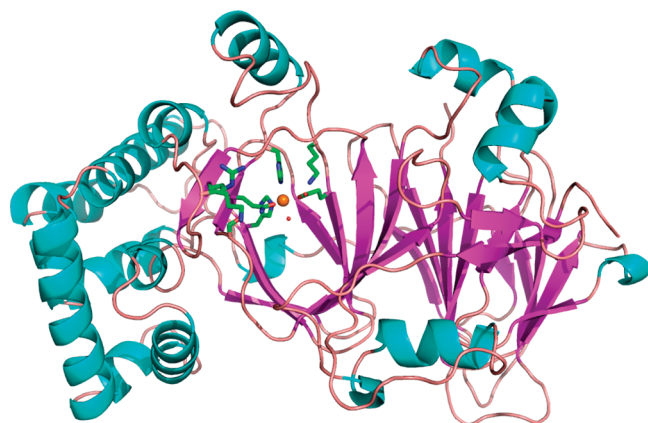


Figure 4. X-ray crystal structure of Type I PMI from *C. albicans* (PDB ID 1PMI).³⁷ α -Helices and β -sheets are depicted in light blue and pink, respectively. Some of the active site residues are represented as sticks in green (C), dark blue (N), and red (O). The zinc cofactor is depicted as an orange large sphere and the zinc-bound water molecule as a small red sphere. PyMOL software⁶² was used to prepare the figure.

below used for a dibase to provide $pK_{\text{a}1}$ and $pK_{\text{a}2}$ values (x_0 being the number of protons on the molecule before base addition)

$$\Delta x = \left(\frac{2[\text{H}^+]^2 + K_{\text{a}1}[\text{H}^+]}{[\text{H}^+]^2 + K_{\text{a}1}[\text{H}^+] + K_{\text{a}1}K_{\text{a}2}} \right) - x_0$$

Graphical representations of Δx as a function of pH for both ligands can be found in the Supporting Information Figure S2.

■ RESULTS AND DISCUSSION

Interactions without Discrete Polarizable Water Molecules. A representation of the three-dimensional structure of Type I PMI from *C. albicans*, obtained from X-ray diffraction by Cleasby et al. (PDB ID code 1PMI),³⁷ is given in Figure 4. Figure 5 displays the structures of the energy-minimized structures of the representative complexes of **1** (A), **2** (B), **3** (C), and **4** (D) with the binding site of PMI. In this binding site, Zn(II) is ligated by Gln111, His113, His285, and Glu138 and the structural water molecule.³⁷ As we previously proposed, upon binding of the substrate or substrate analogue inhibitors, this water mediates the interactions between Zn(II) and the anomeric hydroxyl group of the ligands.¹⁹ The dianionic end of the ligands most likely binds to two cationic residues at the entrance of the cavity, namely Arg304 and Lys310.¹⁸ Table 1 gives the energy balances of the four compounds β -M6P (**1**), α -M6P (**2**), β -G6P (**3**), and β -6DCM (**4**). It lists (a) the values of the energies of the PMI–ligand complexes and their contributions and the energy-minimized values of (b) uncomplexed PMI and (c) uncomplexed ligands, which were separately minimized in the presence of the LC continuum reaction field. The corresponding differences between (a) and the sum of (b) and (c) are listed with the “a” superscript. The overall energy balances, denoted as $\Delta E_{\text{tot}} + \Delta G_{\text{solv}}$, are listed in the last row. In the phosphate series, β -M6P (**1**) has a significantly more favorable energy balance than either α -M6P (**2**) or β -G6P (**3**), by 15.1 and 14.7 kcal/mol, respectively. Such a preference is consistent with the experimental results, which indicate that while β -M6P (**1**) is the PMI substrate, neither α -M6P (**2**) nor β -G6P (**3**) act as substrates and are at best weak inhibitors of ScPMI.^{1,20} The structure of the complex of

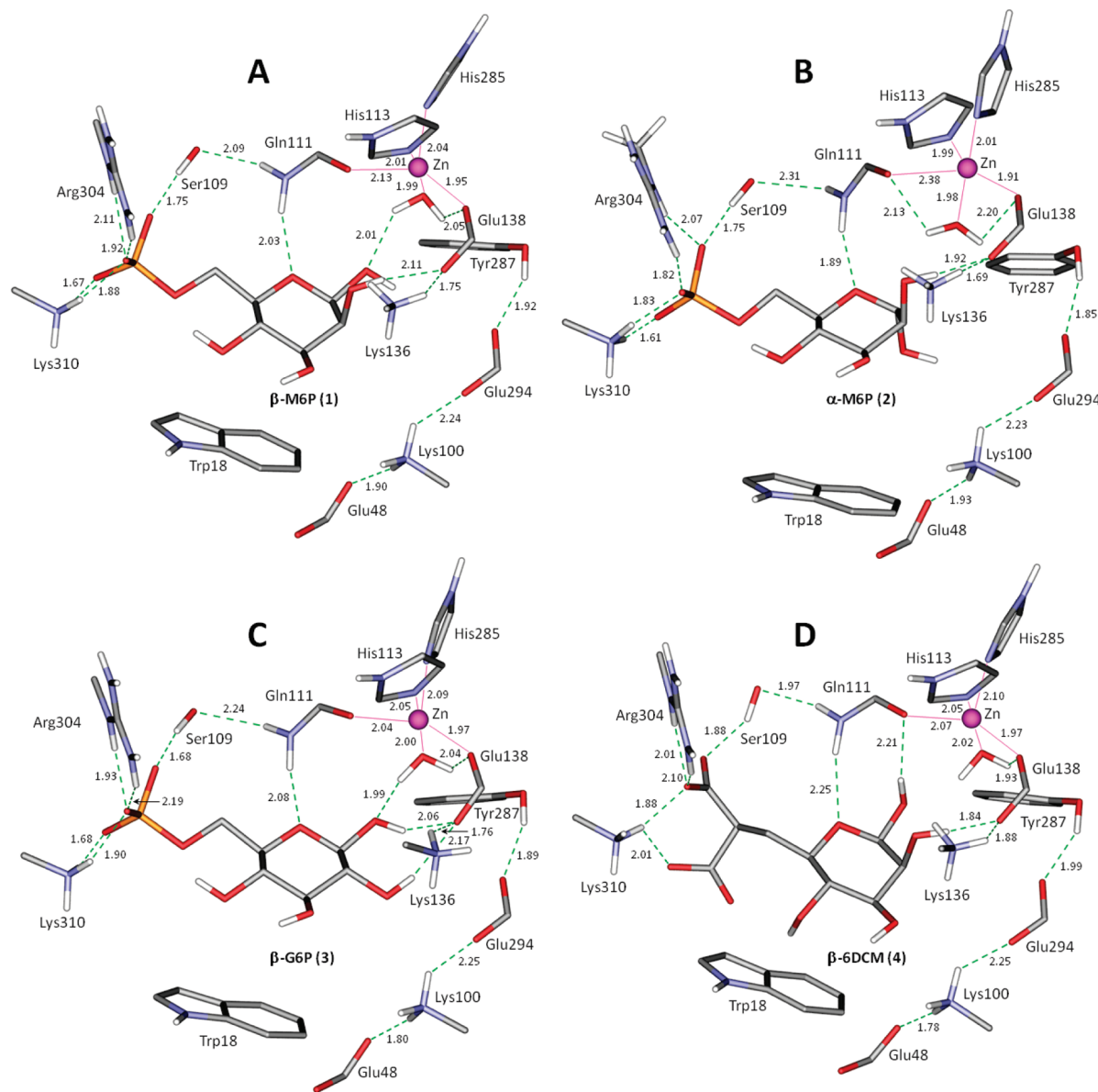


Figure 5. Representation of the complexes of PMI showing only the interactions in the model binding site: (A) with β -M6P (1); (B) with α -M6P (2); (C) with β -G6P (3); (D) with β -6DCM (4).

α -M6P (2, Figure 5B) clearly shows that the anomeric hydroxyl group (linked on C1) is not hydrogen bonded to any active site residue, contrary to β -M6P (1, Figure 5A). On the other hand, the sole consideration of the structure of the complex with β -G6P (3), which is closely similar to that of β -M6P (1), does not enable one to explain the difference in the interaction energies favoring β -M6P. The malonate analogue β -6DCM (4) has a significantly less favorable energy balance than the substrate β -M6P (1), namely by 12.4 kcal/mol. This is contrary to the experimental result showing it to have a 10-fold more favorable binding affinity than β -M6P (1) on ScPMI.¹⁹ These two results can lead to question seriously the accuracy of the potential energy or of some of its contributions. For that purpose, and in keeping with our previous studies,^{18,19} we have sought to validate such energy computations by performing single-point parallel SIBFA and QC computations for the binding of the four ligands to the PMI recognition site involving the same residues for both types of calculations. The structures were extracted from the SIBFA energy-minimized

structures of their complexes with the whole PMI model, and totalling up to 150 atoms. They encompass the end side-chains of Trp18, Glu48, Lys100, Ser109, Gln111, His113, Glu138, Glu294, His285, Arg304, Thr308, and Lys310, and a formamide entity of the backbone at the Thr308-Pro309 junction. The energy results are reported in Table 2. They list the values of the SIBFA interaction energies and their contributions, and the values of the corresponding QC calculations with three different basis sets, namely CEP 4-31G(2d), 6-311G^{**}, and cc-pVT(-f). They also list the values of the LC continuum solvation energies and their electrostatic contributions, along with the corresponding QC/PCM ones (Table 2a). We have also evaluated if the conformational energy rearrangement of the ligands, upon passing for the uncomplexed to the PMI-complexed conformations, δE_{conf} were correctly calculated (Table 2b). The conformation of each uncomplexed ligand was therefore energy-minimized in the presence of the LC continuum reaction field procedure. Single-point QC calculations were done on the PMI-complexed and uncomplexed

Table 1. Values (kcal/mol) of the SIBFA Ligand-PMI Interaction Energies (1: β -M6P, 2: α -M6P, 3: β -G6P, 4: β -6DCM)^a

	PMI-1	PMI-2	PMI-3	PMI-4	PMI	1	2	3	4
E_{MTP}	-7464.2	-7487.1	-7491.1	-7480.1	-7296.1	90.7	87.8	87.2	-0.5
$E_{\text{MTP}}^{\text{a}}$	-258.8	-278.8	-282.2	-183.5					
E_{rep}	6272.6	6289.8	6308.5	6265.6	6070.5	146.9	138.4	148.8	156.8
$E_{\text{rep}}^{\text{a}}$	55.2	80.9	89.2	38.3					
E_1	-1191.6	-1197.3	-1182.6	-1214.5	-1225.6	237.6	226.2	236.0	156.2
E_1^{a}	-203.7	-197.9	-193.0	-145.2					
E_{pol}	-366.0	-364.5	-376.4	-384.6	-366.5	-21.6	-20.4	-24.0	-23.5
$E_{\text{pol}}^{\text{a}}$	22.1	22.4	14.1	5.4					
E_{ct}	-46.3	-45.8	-45.6	-48.6	-42.3	-1.7	-1.3	-1.1	-2.9
E_{ct}^{a}	-2.3	-2.2	-2.2	-3.4					
E_{disp}	-1854.2	-1857.8	-1859.2	-1851.2	-1778.2	-44.2	-43.1	-44.4	-47.9
$E_{\text{disp}}^{\text{a}}$	-31.8	-36.5	-36.6	-25.1					
E_{tor}	454.5	454.5	455.0	453.3	456.0	0.1	0.6	0.5	1.5
$E_{\text{tor}}^{\text{a}}$	-1.6	-2.1	-1.5	-4.2					
ΔE_{tot}	-217.3	-216.3	-219.2	-172.5					
ΔG_{solv}	-3136.6	-3120.0	-3120.3	-3141.0	-3023.8	-244.3	-241.8	-244.6	-216.3
$\Delta G_{\text{solv}}^{\text{a}}$	131.5	145.6	149.1	99.1					
$\Delta E_{\text{tot}} + \Delta G_{\text{solv}}$	-85.8	-70.7	-71.1	-73.4					

^a For a given energy, the values with the “a” superscript are those obtained after subtraction of the uninhibited, energy-minimized protein + isolated inhibitor energies.

conformations. These were done at both HF and MP2 levels. The corresponding conformational energy differences, denoted as $\delta E_{\text{conf}}(\text{HF})$ and $\delta E_{\text{conf}}(\text{MP2})$, respectively, can thus be compared to the SIBFA values without and with the dispersion contribution, namely $\delta E(\text{SIBFA})$ and $\delta E_{\text{conf}}(\text{SIBFA})$. The LC and PCM solvation energies and their electrostatic contributions were compared for the energy-minimized conformations.

The values of $\Delta E(\text{SIBFA})$ are found to be close to their HF counterparts, the relative errors being <3% (Table 2a). While $\Delta E(\text{SIBFA})$ is overestimated with respect with $\Delta E(\text{HF})$ with the CEP 4-31G(2d) and cc-pVTZ(-f) basis sets, it is underestimated with respect to the 6-311G** basis set values. The energy ordering of $\Delta E(\text{HF})$ values 1 > 3 > 2 > 4 is correctly predicted. $\Delta E(\text{SIBFA})$ for the malonate complex PMI-4 is 30 kcal/mol less favorable than for the PMI-1 one. This is consistent with the corresponding $\Delta E(\text{HF})$ differences of 43.5, 35.2, and 42.3 kcal/mol at the CEP 4-31G(2d), 6-311G**, and cc-pVTZ(-f) levels, respectively. Related trends are seen upon inclusion of the E_{disp} contribution in SIBFA and inclusion of correlation in the context of DFT/PBE. The corresponding PMI-4/PMI-1 difference of 38 kcal/mol is consistent with the PBE values of 42.4 and 44.2 kcal/mol with the CEP 4-31G(2d) and cc-pVTZ(-f) basis sets respectively. The numerical values of $\Delta E(\text{SIBFA})$ are larger by 3–4% than the PBE ones. This is consistent with previous results on PMI¹⁷ as well as β -lactamase³⁸ and isopentenyl diphosphate isomerase (IDI)³⁹ metalloenzymes. These showed $\Delta E_{\text{tot}}(\text{SIBFA})$ to be invariably intermediate between the DFT and the MP2 ΔE values. On the other hand, the values of $E_{\text{el}}(\text{solv})/\text{LC}$ compare less favorably to their PCM counterparts, for which the CEP 4-31G(2d), 6-311G**, and cc-pVTZ(-f) basis sets result into similar values. The LC values are underestimated, a feature noted previously.^{17,38} This could be due partly to the fact that in the present LC implementation, no coupling was introduced between the solvent reaction field and the solute induced dipoles. Despite this limitation, a previous study on the binding of a hydroxamate and of a carboxylate inhibitor to PMI had shown

$E_{\text{el}}(\text{solv})/\text{LC}$ to evolve in a consistent manner to $E_{\text{el}}(\text{solv})/\text{PB}$ in a series of nine competing complexes.¹⁷ The $\Delta G_{\text{solv}}(\text{LC})$ values have on the other hand larger values than $E_{\text{el}}(\text{solv})/\text{PCM}$ owing to the additional stabilization due to the summed cavitation and dispersion/repulsion contributions, but the trends are the same as those of $E_{\text{el}}(\text{solv})/\text{LC}$. The overall agreement of $E_{\text{el}}(\text{solv})/\text{LC}$ and $E_{\text{el}}(\text{solv})/\text{PCM}$ is less satisfactory than in the previously investigated complexes.¹⁷ It is noted that $E_{\text{el}}(\text{solv})/\text{LC}$ has a 20 kcal/mol larger magnitude in the PMI-4 complex than in the PMI-1 one, as compared to differences in the 26–29.7 kcal/mol range for $E_{\text{el}}(\text{solv})/\text{PCM}$. Continuum reaction field approaches can have inherent limitations to handle “bare” ionic complexes at the QC, and a fortiori MM, levels. In this connection, the inclusion of nine discrete water molecules, as performed in the next step, will be seen to allow for an improved agreement between QC and MM continuum solvation calculations.

The values of SIBFA conformational energies in the absence of the dispersion contribution, $\delta E(\text{SIBFA})$, reproduce closely the QC/HF ones, $\delta E_{\text{conf}}(\text{HF})$. This is also the case when E_{disp} and correlation are taken into account in the SIBFA and QC calculations, respectively.

Accounting for Discrete Polarizable Water Molecules. Overall the results analyzed in Table 2 validate the essential features of the SIBFA energy calculations and indicate that, since the potential energy function could not be incriminated, the PMI-inhibitor complexes should embody additional factors. Thus a recent study from our Laboratories bore on the complexes of the FAK kinase with five structurally related anionic inhibitors in the pyrrolopyrimidine series, whose affinities ranged from micro- to nanomolar.²² Energy balances in the presence of the sole LC continuum reaction field procedure had similarly failed to rank these inhibitors according to the experimental ordering. By contrast, accounting for and energy-minimizing highly polarized water molecules in the FAK-inhibitor (up to seven for each complex) restored energy balances that were consistent with experiment. Could similar effects be at play in the

Table 2.

	a. Values (kcal/mol) of the SIBFA and QC Interaction Energies in the PMI Model Binding Site			
	PMI-1	PMI-2	PMI-3	PMI-4
E_{MTP}	-1260.5	-1246.6	-1263.3	-1187.6
E_{rep}	328.8	329.6	358.3	302.0
E_1	-931.7	-917.0	-905.0	-885.6
E_{pol}	-142.4	-138.7	-154.5	-155.9
E_{ct}	-44.8	-44.9	-45.8	-47.5
$\Delta E(\text{SIBFA})$	-1118.9	-1100.6	-1105.3	-1088.9
$\Delta E(\text{HF})^a$	-1107.8	-1092.0	-1100.1	-1064.3
$\Delta E(\text{HF})^b$	-1138.1	-1122.0	-1128.8	-1102.9
$\Delta E(\text{HF})^c$	-1112.2	-1096.4	-1104.4	-1069.9
E_{disp}	-105.6	-104.5	-111.2	-97.6
$\Delta E_{\text{tot}}(\text{SIBFA})$	-1224.5	-1205.1	-1216.5	-1186.5
$\Delta E(\text{DFT/PBE})^a$	-1182.5	-1166.9	-1179.3	-1140.1
$\Delta E(\text{DFT/PBE})^c$	-1188.7	-1172.6	-1185.4	-1144.5
$E_{\text{el}}(\text{solv})/\text{LC}$	-192.6	-197.1	-190.0	-213.0
ΔG_{solv}	-265.4	-268.7	-263.1	-290.9
$E_{\text{el}}(\text{solv})/\text{PCM}^a$	-221.6	-233.0		-250.3
$E_{\text{el}}(\text{solv})/\text{PCM}^b$	-220.0	-224.9	-231.2	-246.1
$E_{\text{el}}(\text{solv})/\text{PCM}^c$	-219.2	-223.4	-230.5	-247.8
	b. Conformational and Solvation Energies of the Isolated Ligand			
	1	2	3	4
$\delta E(\text{SIBFA})/\delta E_{\text{conf}}(\text{SIBFA})$	7.0/7.8	10.6/10.5	0.3/0.6	24.5/26.2
$\delta E_{\text{conf}}(\text{HF})^a/\delta E_{\text{conf}}(\text{MP2})^a$	8.1/8.0	11.4/10.9	1.6/1.7	19.9/21.1
$E_{\text{el}}(\text{solvlig/SIBFA})$	-228.8	-225.9	-229.4	-201.0
$\Delta G_{\text{solv}}(\text{LC})$	-242.9	-240.2	-243.4	-214.8
$E_{\text{el}}(\text{solvlig/HF}^a)$	-245.2	-238.9	-251.1	-210.8
$E_{\text{el}}(\text{solvlig/HF}^b)$	-274.4	-270.2	-279.2	-234.9

^a CEP 4-311G** basis set. ^b 6-311G** basis set. ^c cc-pVTZ(-f) basis set.

PMI-inhibitor complexes? We have first considered the PMI-malonate complex (PMI-4), which has three out of four accessible anionic malonate oxygens. One water molecule was bound in an external position to each of them, and its position was energy-minimized. Additional waters were then inserted using the “discrete” software,⁴⁰ interfaced in SIBFA. This software uses a simplified energy function to optimize the location of water molecules around accessible polar sites in a molecular complex. The resulting positions were used as starting points for SIBFA E-M, followed by a short MD simulation (25 ps) resorting as in ref 39 to a simplified version of the SIBFA potential and holding the temperature at 300 K. The final pose was submitted to a last round of E-M. At the outcome of this procedure, each of the three first-shell waters was found to nucleate a network of structured waters, as represented in Figure 6. In the first network, N₁, the first-shell water, W₁, donates a proton to one malonate O, accepts a proton from the amino group of the side-chain of Trp18, and donates its second proton to a second-shell water, W₂. W₂ accepts a second proton from a ligand hydroxyl group and donates a proton to one Glu48 anionic O. Glu48 is itself engaged in a network connecting it to Lys100, Glu294, and Tyr287. The second network, N₂, involves four water molecules. A first-shell water molecule, W₃, accepts a proton from a second-shell one, W₄. W₄ donates its second H to W₅ of a third shell, and W₅ in turn donates one H to one anionic O of the Asp17 residue.

Another first-shell water molecule, W₆, accepts a proton from Lys310, a residue involved as well in the third network. In the third network, N₃, the first-shell water molecule, W₇, donates a proton to a malonate O, accepts a proton from Lys310, and donates its second proton to W₈. W₈ donates one proton to Asp300 and donates the second to W₉. W₉ also donates a proton to Asp300. All three networks are therefore seen to start from one ligand anionic O and to end with one PMI anionic O, which belong, namely, to Asp17, Glu48, Asp300. They thus span three PMI anionic residues that are separated by about 18 Å, far from the actual recognition site. It can also be observed that all molecules or molecular fragments represented in Figure 6 are interconnected by noncovalent bonds. The corresponding complex of 1 is represented in Figure 7. While the water molecules are at similar positions as in the complex of 4, some interactions differ. It is seen in particular that, owing to the lesser accessibility of the phosphate group, the first array no longer starts with an anionic phosphate oxygen, but with Lys310 instead and now involves water W₆.

We report in Table 3 the results after E-M on the first comparative energy balances and their contributions in the PMI-1 and PMI-4 complexes in the presence (A) of the nine water molecules. For comparison, these relative balances are followed by those found upon removal of these waters (B) in the same geometries. It is noted that such values are not identical

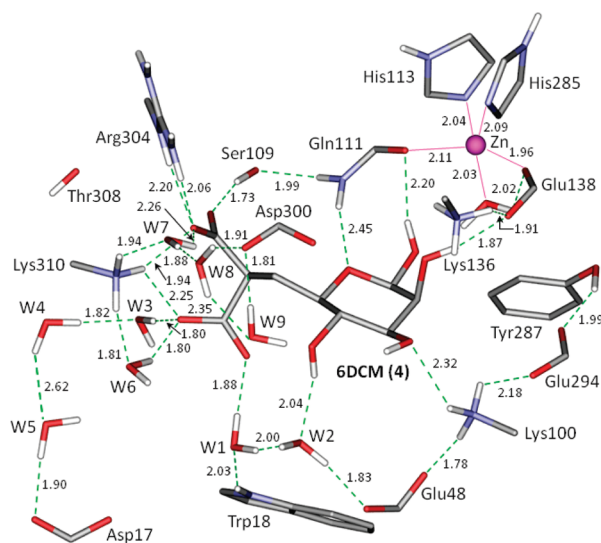


Figure 6. Representation of the complex of PMI with the malonate ligand β -6DCM (4) in the presence of nine structural water molecules.

to those of Table 1, since the structures have been optimized again in the presence of the water molecules. Table 3 also reports the corresponding values in the uncomplexed, energy-minimized PMI, substrate β -M6P (1), and malonate β -6DCM (4) with LC continuum solvation. The energy contributions denoted with a “ δ ” are those found following subtraction of the PMI and corresponding ligand values. For each contribution, the following row of δ values gives the difference in the PMI-1 and PMI-4 complexes, being negative if in favor of the latter. The very large preference of δE_1 in favor of PMI-1 (60.4 kcal/mol) is slightly increased (2.1 kcal/mol) in the presence of the waters. In marked contrast, both polarization and charge-transfer preferences in favor of the malonate complex are significantly enhanced in their presence, passing from -17.1 to -25.8 kcal/mol for δE_{pol} and from -1.4 to -6.3 kcal/mol for δE_{ct} . The δE_{disp} preference in favor of PMI-1 is reduced by 5 kcal/mol from 6.0 to 1.0 in the presence of the nine waters. The results of Table 3 indicate that the nine discrete water molecules preferentially stabilize the PMI-malonate complex than the PMI–substrate complex. This stabilization originates from polarization (-8.7 kcal/mol), charge-transfer (-4.9 kcal/mol), and dispersion (-5.0 kcal/mol). At this stage, the final relative energy balances continue to favor PMI-1 over PMI-4, although the energy difference of 4.3 kcal/mol is considerably reduced compared to its value in the absence of the discrete waters, namely 14.1 kcal/mol.

It was thus essential at this point to validate again the SIBFA results, now regarding the amount of stabilization due to the water molecules. This was done by parallel QC computations in new model binding sites, extracted from ongoing energy-minimizations of the PMI-1 and PMI-4 complexes, and now augmented with the carboxylate side-chains of Asp17 and Asp300 in both QC and SIBFA calculations. The results are reported in Table 4. Table 4 also give the ΔE values upon removal of the nine water molecules. For each energy contribution, and for each ligand, we list the value of $\delta(A-B)$, the energy gain contributed by the waters. For E_1 , $\delta(A-B)$ is only -1.6 kcal/mol more in favor of PMI-4 compared to PMI-1 (Table 4a). For E_{pol} and E_{ct} , these differences raise up to -7.7 and -5.2 kcal/mol, respectively. E_{disp} contributes a slightly smaller relative stabilization of -4.6

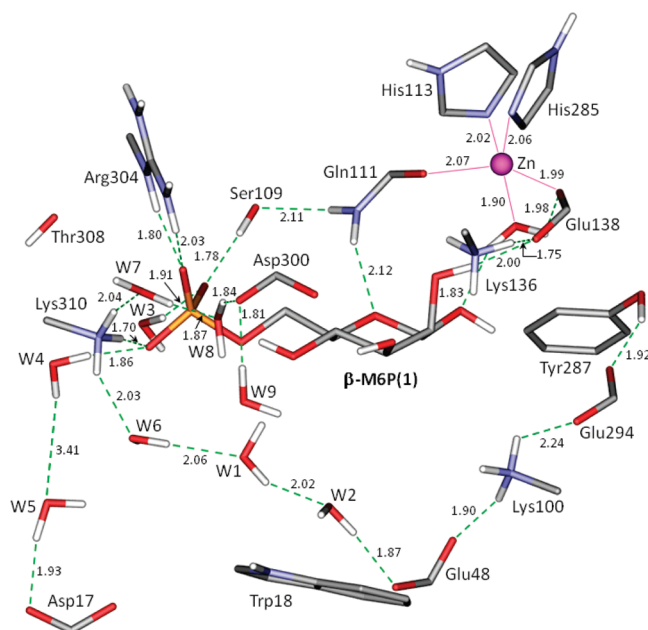


Figure 7. Representation of the complex of PMI with the substrate β -M6P (1) in the presence of nine structural water molecules.

kcal/mol (Table 4b). These values are consistent with those found in the complete PMI-ligand complexes. The QC calculations were performed with the CEP 4-31G(2d) and the cc-pVTZ(-f) basis sets. The values of $\Delta E(\text{SIBFA})$ are for the three ligands seen to match closely the QC ones for both (A) and (B) computations, with relative errors $\leq 2\%$ (Table 4a). It is essential to observe that the total stabilization energies brought by the water molecules are close in the $\Delta E(\text{SIBFA})$ and $\Delta E(\text{QC})$ computations. Thus, for $\Delta E(\text{SIBFA})$, they amount to -121.7 and -136.1 kcal/mol for the substrate (PMI-1) and malonate (PMI-4) complexes, respectively. The corresponding $\Delta E(\text{QC})^a$ values are -123.0, and -138.7 kcal/mol. The $\Delta E(\text{QC})^b$ values are on the other hand larger, namely -130.0 and -145.8 kcal/mol. Nevertheless it is noteworthy that the PMI-4 stabilization values with respect to PMI-1 are all very consistent: -14.4 from $\Delta E(\text{SIBFA})$, -15.7 from $\Delta E(\text{QC})^a$, and -15.8 from $\Delta E(\text{QC})^b$. Table 4a also lists the results at the HF level with the more complete cc-pVTZ basis set upon adding a 3d polarization function on H atoms, a 4f one on C, N, O, and P atoms, and a 5g one on Zn(II) with the corresponding exponents.³³ This is seen to affect by <1 kcal/mol out 1100 the HF interaction energies computed at the cc-pVTZ(-f) level. The SIBFA/QC comparisons were extended to the correlated DFT/PBE level upon including the dispersion contribution in SIBFA (Table 4b). The trends of $\Delta E_{\text{tot}}(\text{SIBFA})$ are consistent with the DFT ones concerning the four complexes. $\Delta E_{\text{tot}}(\text{SIBFA})$ has now 4 and 3% larger magnitudes than the $\Delta E(\text{DFT}/\text{PBE})$ values with the CEP 4-31G(2d) and cc-pVTZ(-f) basis sets, respectively. Such a relative overestimation is consistent with previous results on a series of related model complexes in metallo- β -lactamase³⁸ and the IDI Zn/Mg metalloenzymes,³⁹ where $\Delta E_{\text{tot}}(\text{SIBFA})$ had magnitudes consistently intermediate between the DFT and the MP2 ones. This was ascribed to an underestimation of dispersion effects in DFT and an overestimation of the stabilization from MP2 due to Basis Set Superposition Error (BSSE) effects. As was the case at the HF level, it is observed that a closer agreement is

Table 3. Values (kcal/mol) of the SIBFA Interaction Energies with PMI (A) with and (B) without the Nine Structural Waters^a

	PMI-1 (A)	PMI-4 (A)	PMI-1 (B)	PMI-4 (B)	PMI	1	4
E_1	-1285.6	-1304.5	-1190.8	-1211.8	-1225.6	237.6	156.2
δE_1	-297.6	-235.1	-202.8	-142.4			
δ	62.5		60.4				
E_{pol}	-399.2	-426.9	-364.4	-383.4	-366.5	-21.6	-23.5
δE_{pol}	-11.1	-36.9	23.7	6.6			
δ	-25.8		-17.1				
E_{ct}	-61.4	-68.9	-45.8	-48.4	-42.3	-1.7	-2.9
δE_{ct}	-17.4	-23.7	-1.8	-3.2			
δ	-6.3		-1.4				
E_{disp}	-1899.0	-1901.7	-1852.7	-1850.4	-1778.2	-44.2	-47.9
δE_{disp}	-76.6	-75.6	-30.3	-24.3			
δ	1.0		6.0				
$\delta E(\text{SIBFA})$	-402.7	-371.3	-211.2	-163.3			
$\delta \delta E(\text{SIBFA})$	31.4		47.9				
ΔG_{solv}	-3126.0	-3125.0	-3140.1	-3145.8	-3023.8	-242.9	-214.8
$\delta \Delta G_{\text{solv}}$	140.7	113.6	126.6	92.8			
$\delta \delta \Delta G_{\text{solv}}$	-27.1		-33.8				
$\delta \delta E(\text{SIBFA}) + \delta \delta \Delta G_{\text{solv}}$	4.3		14.1				

^a The energy contributions denoted with a “ δ ” are those found following subtraction of their values in uncomplexed, separately energy-minimized PMI and ligand. The following δ values are the differences of the corresponding contribution in the β -M6P (**1**) and β -6DCM (**4**) complexes.

found for SIBFA with the cc-pVTZ(-f) basis set than with the CEP 4-31G(2d) basis set, even though SIBFA resorts to distributed multipoles and polarizabilities derived from CEP 4-31G-(2d) calculations on the individual fragments. The relative stabilization energies brought by the waters are again consistent. Thus in SIBFA they amount to -158.4 and -177.4 kcal/mol for the substrate and malonate complexes, respectively. The corresponding DFT values are -147.7 and -169.9 kcal/mol with the CEP 4-31G(2d) basis set and -155.0 and -177.0 kcal/mol with the cc-pVTZ(-f) basis set. The relative water-contributed stabilizations amount thus to -19.0 with SIBFA and to -22.2 and -22.0 kcal/mol with the CEP 4-31G(2d) and cc-pVTZ(-f) basis sets, respectively. Finally Table 4c gives the values of the continuum solvation energies, namely E_{el}/LC and $\Delta G_{\text{solv}}/\text{LC}$ as compared to those of $E_{\text{el}}(\text{PCM})$ using the CEP 4-31G(2d) and cc-pVTZ(-f) basis sets. The numerical agreement between the LC and PCM $E_{\text{el}}(\text{solv})$ values improves significantly in the presence of the discrete waters. The difference of continuum solvation energies between the PMI-1 and PMI-4 complexes is reduced in their presence. A further reduction could be anticipated when the malonate and phosphate groups are in addition to these waters shielded by the residues of the complete protein.

Final Tentative Energy Balances. The favorable outcome of such validations led us to reconsider the energy balances by seeking for an improved representation of the solvation energies of the uncomplexed ligands. This was done by inclusion of explicit structural water molecules. It is in line with the proposal for a “discrete-continuum” procedure, which was first put forth by Claverie et al.⁴⁰ A pioneering study by Pullman et al.⁴¹ had shown that the monoanionic phosphate group exerts very strong structuring effects on waters in its first hydration shell, and that these effects could extend to the second shell. Such effects should be significantly amplified with ligands having dianionic moieties. Because in solution, the phosphate (β -M6P, **1**) ligand has three accessible anionic oxygens while the malonate ligand (β -6DCM,

4) has four, different numbers of first- and second-shell waters are anticipated. However, for these models to be consistent, both ligands should be solvated by an equal number of waters. We were thus led to solvate both in a box of 64 water molecules. This box was initially created by the Accelrys software⁴² with the ligand in the center. The waters were first relaxed by energy-minimization using Accelrys. E-M was subsequently resumed by SIBFA. It was followed by molecular dynamics (MD) at constant temperature using as in ref 39 a simplified version of the SIBFA potential with scalar instead of anisotropic polarizabilities and no charge transfer. MD was rerun until no significant improvement of the total energies took place, namely 1.5 kcal/mol out of 600 over 0.5 ns production and 0.5 kcal/mol in the last 20 ps. The last frame was in turn submitted to E-M. In an alternative route, MD followed by E-M was done starting from a structure minimized by the Accelrys software. Finally, the last simulations permuted the water shells of **1** and **4**, and E-M was performed subsequently. The present search can by no means sample the energy surface but should enable one to evaluate the amount of actual **1** versus **4** solvation energy differences as compared to a pure continuum approach. Interestingly, two different structures (I and II) were obtained for malonate structure **4-64W**. The first has a less favorable intramolecular (conformational) energy, but a more favorable intermolecular interaction energy with water than the second, so that both differed in terms of their total energies by <0.9 kcal/mol out of 300. Both will be used as energy zero for component “c” of the final energy balances which will be given thereafter. We have validated the values of the interaction energies by parallel single-point QC calculations on the best solvated **1-64W** structure and the two competing solvated **4-64W** ones. The interaction energies are computed as the differences between the total energies of, on the one hand, the solvated complex and, on the other hand, those of the ligand in its solvated conformation and 64 times that of a water molecule. The results are given in Table 5. The SIBFA differences in **4-64W** versus

Table 4.

a. Values (kcal/mol) of the SIBFA and QC Interaction Energies in the PMI Model Binding Site Extracted from the Energy-Minimized PMI Complex (A) with and (B) without the Nine Polarizable Waters				
	A		B	
	PMI-1	PMI-4	PMI-1	PMI-4
E_{MTP}	-1453.8	-1437.0	-1272.8	-1223.8
E_{rep}	411.6	433.4	312.4	303.6
E_1	-1042.1	-1003.5	-960.4	-920.2
$\delta E_1(\text{A-B})$	-81.7	-83.3		
E_{pol}	-176.0	-190.4	-152.1	-158.8
$\delta E_{\text{pol}}(\text{A-B})$	-23.9	-31.6		
E_{ct}	-59.9	-68.3	-43.9	-47.1
$\delta E_{\text{ct}}(\text{A-B})$	-16.0	-21.2		
$\Delta E(\text{SIBFA})$	-1278.1	-1262.2	-1156.4	-1126.1
$\delta E(\text{A-B})$	-121.7	-136.1		
$\Delta E(\text{HF})^a$	-1268.2	-1243.0	-1145.2	-1104.3
$\delta E(\text{A-B})^a$	-123.0	-138.7		
$\Delta E(\text{HF})^b$	-1278.9	-1253.1	-1148.9	-1107.3
$\delta E(\text{A-B})^b$	-130.0	-145.8		
$\Delta E(\text{HF})^c$	-1279.5	-1252.7	-1150.1	-1107.7
$\delta E(\text{A-B})^c$	-129.4	-145.0		

b. $\Delta E(\text{SIBFA})$ with E_{disp} and Correlated $\Delta E(\text{DFT/PBE})$ Results (A) with and (B) without the Nine Polarizable Waters				
	A		B	
	PMI-1	PMI-4	PMI-1	PMI-4
E_{disp}	-139.8	-138.7	-103.1	-97.4
δE_{disp}	-36.7	-41.3		
$\Delta E_{\text{tot}}(\text{SIBFA})$	-1417.9	-1400.9	-1259.5	-1223.5
$\delta E(\text{A-B})$	-158.4	-177.4		
$\Delta E(\text{DFT/PBE})^a$	-1368.0	-1348.9	-1220.3	-1179.0
$\delta E(\text{A-B})^a$	-147.7	-169.9		
$\Delta E(\text{DFT/PBE})^b$	-1382.0	-1362.3	-1227.0	-1185.3
$\delta E(\text{A-B})^b$	-155.0	-177.0		

c. Values of the Continuum Solvation Energies (A) with and (B) without the Nine Polarizable Waters				
	A		B	
	PMI-1	PMI-4	PMI-1	PMI-4
$\Delta G_{\text{solv}}/\text{LC}$	-387.8	-392.1	-399.2	-416.5
E_{el}/LC	-281.2	-283.2	-316.6	-329.5
$E_{\text{el}}/\text{PCM}^a$	-283.7	-292.7	-340.0	-355.1
$E_{\text{el}}/\text{PCM}^b$	-281.7	-290.3	-338.2	-353.7

^a CEP 4-31G** basis set. ^b cc-pvTZ(-f) basis set. ^c cc-pvTZ basis set.

1-64W solvation energies are in the range 39–52 kcal/mol and in the range 65–77 kcal/mol without and with E_{disp} , respectively. Such values are notably larger than those found with the LC continuum reaction field (Table 2), which amount to 28.8 kcal/mol. With the CEP 4-31G(2d) basis set, the corresponding QC difference is in the range 49–65 kcal/mol at the HF level and 57–72 kcal/mol at the DFT-D level. These QC values for 4-64W versus 1-64W solvation energies are, similarly to the SIBFA case, larger than found with the PCM computation, of 34.4 kcal/mol with the CEP 4-31G(2d) basis set. This clearly indicates the need for explicit water molecules to account for solvation energies of ligands with a dianionic charge. It is noted that $\Delta G_{\text{solv}}(\text{LC})$ of the

malonate and phosphate-64W complexes are equal to within <1 kcal/mol. This translates the fact that the dianionic charges of the two ligands are virtually equally shielded by the water shells. With respect to the HF calculations, $\Delta E(\text{SIBFA})$ appears to underestimate the $\Delta E(\text{HF})$ solvation energy differences of 4-64W versus 1-64W by about 10 kcal/mol out of 600. While this represents a small relative amount (<2%), it could be prejudicial to the energy balances. However it is also seen from Table 4 that the corresponding differences of malonate 4 versus phosphate 1 $\Delta E(\text{SIBFA})$ values in the PMI model binding site are underestimated by a similar amount. This should enable for consistency in such balances. On the other hand, $\Delta E_{\text{tot}}(\text{SIBFA})$ gives

Table 5. Values (kcal/mol) of the SIBFA and QC(HF) Interaction Energies in the Complexes of β -M6P (**1**) and β -6DCM (**4**) Derivatives with 64 Water Molecules (**I** and **II** Are Two Conformations of 4-64W)

	1-64W	4-64W (I)	4-64W (II)	Water box
E_{MTP}	-1205.4	-1106.4	-1118.2	-907.2
E_{rep}	899.7	836.3	845.1	794.4
E_1	-305.8	-270.1	-273.1	-112.8
E_{pol}	-235.3	-219.5	-226.6	-217.9
E_{ct}	-117.5	-116.0	-119.7	-115.5
$\Delta E(\text{SIBFA})$	-658.5	-606.5	-619.3	-446.2
$\delta/1-64W$		52.0	39.2	212.3
ΔG_{solv}	-279.3	-279.1	-279.7	
$\Delta E(\text{HF})^a$	-672.0	-607.0	-622.7	-461.6
$\delta/1-64W$		65.0	49.3	210.4
$\Delta E(\text{HF})^b$	-721.8	-653.6	-666.9	-502.8
$\delta/1-64W$		68.2	54.8	
E_{disp}	-357.2	-331.6	-330.9	-278.2
$\Delta E_{\text{tot}}(\text{SIBFA})$	-1015.7	-938.6	-950.2	-724.2
$\delta/1-64W$		77.1	65.5	291.5
$\Delta E(\text{B3LYP})^a$	-865.0	-792.5	-809.9	-646.5
$\delta/1-64W$		72.5	55.1	218.0
$\Delta E(\text{DFT-D})^a$	-977.1	-904.8	-919.8	-717.7
$\delta/1-64W$		72.3	57.2	259.4

^a CEP 4-31G(2d) basis set. ^b cc-pvtz(-f) basis set.

rise to differences of 4-64W versus 1-64W solvation energies that are about 5–8 kcal/mol out of 900 larger than the DFT-D ΔE_{solv} values, rather than being smaller as at the HF level. These differences amount to 77.1 and 65.5 kcal/mol for I and II from SIBFA while they amount to 72.3 and 57.3 kcal/mol, respectively, in DFT-D. It is not possible presently to evaluate the difference between **1** and **4** interaction energies in the PMI binding site, owing to the unavailability of DFT-D Zn(II) parameters. The fact that $\Delta E_{\text{tot}}(\text{SIBFA})$ is larger in magnitude than $\Delta E(\text{DFT-D})$ could imply that a rescaling of E_{disp} should be considered in future studies along with the use of correlated multipoles and polarizabilities. This is planned for future studies but should not affect the essential conclusions reached in this work regarding the role of polarizable waters.

Table 6 reports the final energy balances in which the desolvation energies of the inhibitors are computed with the shell of 64 water molecules. The energy balances, δE , are written as follows: $\delta E = \mathbf{a} - \mathbf{b} - \mathbf{c} + \mathbf{d}$. In this expression, **a** is the energy-minimized value of the PMI-inhibitor complex; **b** is the energy-minimized value of the uncomplexed ligand in a box of 64 water molecules; **c** is the energy-minimized value of unligated PMI with the 9 water molecules; and **d** is the energy-minimized value of a 64-water box. The values of the difference are given for each contribution with the superscript “a”. The final energy balances are seen to favor the PMI-4 complex over PMI-1 complex by a very large amount, namely 36 kcal/mol. In marked contrast to the outcome of **d**, E_1^a is found to strongly disfavor PMI-4 with respect to PMI-1, namely by 33–42 kcal/mol. The initial balances using the sole LC continuum reaction field procedure (Table 1) gave an even larger difference, namely 58.5 kcal/mol. The trends in E_1^a are opposed by those of E_{pol}^a , E_{ct}^a , and E_{disp}^a , which favor PMI-4 over PMI-1 by 38–46, 5–7.5, and 24–26 kcal/mol, respectively. In fact, E_{pol}^a is positive in the case of

PMI-1. This was noted in the initial energy balances with the sole LC continuum for all ligands. In the present case, it has two causes: with the nine waters, E_{pol} is more stabilizing for the PMI-4 complex than for the PMI-1 one; and conversely, E_{pol} has stronger values (10–18 kcal/mol) in **1**-64W than in **4**-64W. Destabilizing E_{pol} balances were previously found for the complexes of PMI with SPAH and SPAA inhibitors.¹⁷ This was also found in a recent study using the AMOEBA polarizable force-field concerning the complex of trypsin with ligands.^{43,44} The fact that E_{disp}^a also favors PMI-4 over PMI-1 stems from its much more favorable value in **1**-64W than in **4**-64W as seen from Table 5.

As in ref 22, an indication of the very strong polarization of the discrete waters in networks N1–N3 is given by the values of their total dipole moments. Thus for the malonate complex PMI-4, all nine waters have dipole moments in the range 2.65–3.15 D, and six have dipole moments larger than the value of 2.7 D found in icelike arrangements, as computed using SIBFA and the CEP 4-31G(2d) multipoles and polarizabilities.³² These are W_8 (3.15D), W_7 (2.82D), W_2 (2.82D), W_3 , W_6 and W_9 (2.75D). This is the case in the substrate complex PMI-1 for only four of them.

Two important issues raised by the present treatment, which will have to be addressed in future studies, are (a) the large and positive (destabilizing) energy balance for the complexation of **1**, amounting to 20 kcal/mol; (b) an overestimated preference favoring **4** over **1**, amounting to 35 kcal/mol. Regarding (a), limiting in the PMI complexes the number of discrete water molecules to nine is expected to weaken the weight of component **a** of the energy balances, since both **1** and **4** contribute an additional net charge of -2 to the net charge of the uncomplexed PMI model, which is of -3. Additional waters solvating W_1 – W_9 in outer layers and in accessible zones of PMI would undergo the large electrostatic potential and field contributed by the ligands, more so than a continuum solvation model. They should on the other hand, have a limited impact on the relative PMI-1 and PMI-4 ΔE_{tot} values due to their increased distances to the target PMI-1 and PMI-4 sites. This can be assessed upon comparing the values of ΔG_{solv} in the two complexes, since this quantity could be taken as an indicator of the long-range effect exerted by the solute potential on the solvent. Thus the two ΔG_{solv} values differ by only 1 kcal/mol out of 3130, while they differed by 5 kcal/mol in favor of PMI-4 in the absence of the discrete waters. We have evaluated the extent to which accounting for these long-range effects could impact the energy balances, by limiting to 27 the number of waters solvating **1** to compute component **c** of the energy balance, the ligand desolvation energy. This number corresponds to three first-shell waters around each of the three anionic O atoms of **1**, each water molecule in turn solvated by two second-shell waters. Similarly component **d** of the energy balance, the water–water solvation energy, was recomputed with 27 water molecules. After $E_{\text{-M}}$, the values of ΔE_{tot} and ΔG_{solv} for **1**-27W are -341.0 and -203.5 kcal/mol, respectively. The corresponding values for 27W are -285.4 and -93.0 kcal/mol. This results for PMI-1 into a less severe positive balance δE , now amounting to 10.4 kcal/mol instead of 20.4. It indicates that the numerical values of δE are sensitive to the number of discrete solvation waters, although the search for a balanced and realistic number of discrete waters handling “on par” components **a**–**d** remains to be done. There is an additional factor which could render the δE values more stabilizing. It is the entropy associated with the discrete waters of the solvated

Table 6. Values (kcal/mol) of the SIBFA Ligand-PMI Interaction Energies in the Presence of Nine Polarizable Water Molecules (Component **a**; **1**, β -M6P; **4**, β -6DCM)^a

	a	a	b	b	c	d
	PMI-1	PMI-4	1-64W	4-64W	PMI	64W
E_{MTP}	-7657.5	-7707.7	-1089.5	-1094.0/-1092.8	-7497.5	-907.2
$E_{\text{MTP}}^{\text{a}}$	+22.3	-23.4/-24.6				
E_{rep}	6371.9	6403.2	1040.3	983.4/991.5	6165.3	794.4
$E_{\text{rep}}^{\text{a}}$	-39.3	48.9/40.8				
E_1	-1285.6	-1304.5	-49.3	-110.6/-101.2	-1332.2	-112.8
E_1^{a}	-16.9	25.5/16.2				
E_{pol}	-399.2	-426.9	-258.1	-240.0/-247.5	-400.5	-217.9
$E_{\text{pol}}^{\text{a}}$	+41.5	-4.3/3.6				
E_{ct}	-61.4	-68.9	-117.9	-117.9/-120.0	-59.8	-115.5
E_{ct}^{a}	0.8	-6.7/-4.6				
E_{disp}	-1899.0	-1901.7	-400.4	-378.7/-376.9	-1817.8	-278.0
$E_{\text{disp}}^{\text{a}}$	+41.2	16.8/15.0				
E_{tor}	454.4	453.4	0.2	0.9/0.2	455.8	
$E_{\text{tor}}^{\text{a}}$	-1.6	-3.3/-2.6				
ΔE_{tot}	+64.9	28.0/27.6				
ΔG_{solv}	-3126.0	-3125.0	-279.3	-279.1/-279.7	-3006.8	-204.6
$\Delta G_{\text{solv}}^{\text{a}}$	-44.5	-43.7/-43.1				
$\Delta E_{\text{tot}} + \Delta G_{\text{solv}}$	+20.4	-15.7/-15.5				

^a For a given energy or energy contribution, the values with the "a" superscript are those obtained after subtraction of the corresponding ones in (i) the unligated, energy-minimized protein with nine water molecules (component **b**), (ii) the uncomplexed, energy-minimized ligand in a bath of 64 water (W) molecules (component **c**), and addition of (iii) an energy-minimized bath of 64 water molecules (component **d**).

complexes which is not presently taken into account to compute components **a**–**d** of δE , particularly **c** and **d**. The dianionic charges of **1** and **4** exerting a much greater ordering effect on the first- and second-shell waters in the **1**-64W and **4**-64W complexes than in 64W, entropy should accordingly favor the latter. Following its inclusion, component **d** of the energy balance should exert a greater stabilizing effect than the destabilizing effect of component **c**. The need to include entropy effects is also necessary regarding the second above-mentioned issue. In this respect concerning issue (b), the difference of solvation energies between **1**-64W and **4**-64W is possibly overestimated owing to the absence of entropy effects, since these could be larger in **4**-64W than in **1**-64W. This is because malonate has two rotatable bonds for the conformation of the terminal dianionic chain, namely around each C–C_{Oani} bond, while **1** has only one, around the O_{est}–P bond. The rotations around two C–C_{Oani} bonds of **4** are expected to thermalize more the water layers than that around the single O_{est}–P bond of **1**. Thus entropy should reduce the difference of solvation energies of **1** and **4**. Overestimation of the difference of solvation energies between **1**-64W and **4**-64W are unlikely to originate from pK_a effects. Indeed, pK_{a1} and notably pK_{a2} values of the phosphate (**1**) and malonate (**4**) ligands are not significantly different. The values were accurately determined in water by plotting the number of exchanged protons as a function of pH to yield respectively 1.86 ± 0.01 and 6.84 ± 0.01 for β -M6P (**1**), and 2.95 ± 0.02 and 6.39 ± 0.02 for β -6DCM (**4**). Consequently, both compounds are expected to display comparable repulsive interactions between the two anionic oxygens of the phosphate and the malonate groups. The corresponding energy terms, **b** and **d**, are equal for all ligands, so that the outcome of their more detailed evaluations should not impair the relative energy

balances. It is noted that entropy effects in the **1**-64W and **4**-64W complexes would in any case further aggravate the outcome of the energy balances obtained with the sole continuum approach, since these already disfavor malonate by 12.4 kcal/mol. Therefore they should not affect the essential conclusions of this study, namely, (a) the presence of networks of highly polarized water molecules around the dianionic entity of PMI ligands at the enzyme active site is indispensable for meaningful relative energy balances; and (b) polarization and charge-transfer are major contributors in such balances.

CONCLUSIONS AND PERSPECTIVES

We have in this study compared the relative energy balances for the complexation of the Zn-metalloenzyme Type I PMI from *C. albicans* by four ligands in the mannose series. The first three β -M6P (**1**), α -M6P (**2**), and β -G6P (**3**) have in common a dianionic 6-phosphate. The fourth, β -6DCM (**4**), has in **1** phosphate replaced by malonate. This compound was designed as a substrate analogue PMI inhibitor in order to improve the resistance against enzymatic cleavage and the bioavailability. We first computed solvation/desolvation effects using the LC continuum reaction field procedure. The relative energy balances have correctly accounted for the preferential binding of **1** over its **2** and **3** isomers, but failed to account for the preferential binding of malonate **4** over **1**. This led us to search for improved models of the PMI-inhibitor/substrate complexes, upon including explicit, discrete water molecules. The presence of three networks of highly polarized water molecules was identified at the outcome of energy-minimization. Each network originates with one water solvating one of the three accessible anionic ligand oxygens at the entrance of the cavity. These networks also solvate

Arg304/Lys310 and extend to anionic PMI residues, namely Asp17, Glu48, Asp300, which are remote from the ligand binding site. Relative energy balances including such waters, and computing the ligand desolvation energies in a box of 64 water molecules, resulted into a very large (36 kcal/mol) preference now favoring malonate **4** over substrate **1**. The polarization, charge-transfer, and dispersion contributions were found to be critical contributions of such a preference.

An essential feature of this and of previous^{17,22,38} studies is the validation of the SIBFA results by comparison with ab initio QC calculations on complexes representing the recognition site. These were extracted from the energy-minimized large PMI-ligand simulations, and encompassed up to 200 atoms. The values of the SIBFA intermolecular interaction energies were found to match the QC ones with relative errors <3%. They also reproduced very closely the amounts of energy stabilization brought by the nine structural waters.

Along with a preceding work, bearing on the binding of five competing anionic inhibitors to FAK kinase,²² in line with results from refs 43 and 44 and to the best of our knowledge, the present work constitutes the first explicit demonstration of the onset of two interwoven effects: (a) the need for a limited number of discrete water molecules; (b) the decisive effects on the relative energy balances of polarization and charge-transfer as contributed by such waters. For ligand-macromolecule complexes, and in the context of polarizable molecular mechanics/dynamics, a simple criterion could be proposed to identify discrete as opposed to "bulk" waters. It is the value of the total dipole moment of the considered water as compared to that in ice. Six and four water molecules in the malonate PMI-4 and substrate PMI-1 complexes respectively were found to fulfill this criterion, having dipole moments in the range 2.7–3.2 D; the dipole moment of a water molecule in an icelike arrangement, as computed with the CEP 4-31G(2d) multipoles and polarizabilities, is of 2.7 D.⁴⁵

Recent review papers have highlighted the issues remaining to be solved toward addressing the energetics of ligand-macromolecule interactions.^{46–49} Along with the actual force-field accuracy, these concern the weight of entropy,⁵⁰ the role of bound waters,^{51–54} extent of sampling, as well as possible variations in protonation.⁵⁵ Specifically, the present and our preceding²² study aim at quantifying the ΔH contributions due to networks of bound waters originating in the ionic sites of the recognition complex. Presently, the relative PMI-4 versus PMI-1 stabilization energy is too large, and it will be critical for future studies to attempt to explicitly embody entropy effects for the ligand-protein complexes as well as for the uncomplexed, solvated ligands and the protein. Following E-M, these complexes are held in place on the one hand by a water-mediated interaction of the mannose ring with Zn(II) and on the other hand by ionic H-bonds of the dianionic moiety with Arg304 and Lys310. This should confer rigidity to the structure. Therefore evaluation of vibration and configurational entropy by a harmonic analysis could be envisaged.^{56–58} A first step toward this direction is taken upon including the vibrational contribution to entropy (work in progress). Such an analysis, however, could not be envisaged in the case of the uncomplexed, solvated ligands and proteins owing to the multiple-minima issue. Extensive sampling with Monte Carlo or molecular dynamics appears then to be mandatory. However for consistency and on account of the dominant role of polarization, these could only be considered in the framework of polarizable molecular mechanics/dynamics.

The conclusions of the present study are a strong incentive to go toward developing free energy calculation capabilities within the context of the SIBFA approach: work is in progress along these lines.

■ ASSOCIATED CONTENT

S Supporting Information. Titration curves of β -M6P (**1**) and β -6DCM (**4**) by NaOH (0.02 M). This material is available free of charge via the Internet at <http://pubs.acs.org>.

■ AUTHOR INFORMATION

Corresponding Author

*E-mail: nohad.gresh@parisdescartes.fr.

■ ACKNOWLEDGMENT

The computations mentioned in this work were performed using resources from GENCI (CINES/IDRIS), Grant 2009-075009, and of the Centre de Ressources Informatiques de Haute Normandie (CRIHAN, Rouen, France). N.G. wishes to thank Drs. David Perahia, Michael K. Gilson, William C. Swope, and Jed Pitera for fruitful discussions regarding the computation of entropy effects in molecular mechanics/dynamics. Dr. Yu Wei Lu (Laboratoire de Chimie-Physique, Univ Paris-Sud) is also gratefully acknowledged for helpful discussions regarding acid-base titrations.

■ REFERENCES

- (1) Rose, I. A.; O'Connell, E. L.; Schray, K. J. *J. Biol. Chem.* **1973**, *248*, 2232–2234.
- (2) Schray, K. J.; Waud, J. M.; Ehrhardt Howell, E. *Arch. Biochem. Biophys.* **1978**, *189*, 106–108.
- (3) Malaisse-Lagae, F.; Willem, R.; Penders, M.; Malaisse, W. *J. Mol. Cell. Biochem.* **1992**, *115*, 137–142.
- (4) Tanner, W.; Lehle, L. *Biochim. Biophys. Acta* **1987**, *906*, 81–99.
- (5) Collins, L. V.; Attridge, S.; Hackett, J. *Infect. Immun.* **1991**, *59*, 1079–1085.
- (6) Smith, D. J.; Proudfoot, A. E. I.; Friedli, L.; Klig, L. S.; Paravicini, G.; Payton, M. A. *Mol. Cell. Biol.* **1992**, *12*, 2924–2930.
- (7) Jensen, S. O.; Reeves, P. R. *Biochim. Biophys. Acta* **1998**, *1382*, 5–7.
- (8) Payton, M. A.; Rheinheimer, M.; Klig, L. S.; DeTiani, M.; Bowden, E. *J. Bacteriol.* **1991**, *173*, 2006–2010.
- (9) Smith, D. J.; Proudfoot, A. E. I.; De Tiani, M.; Wells, T. N. C.; Payton, M. A. *Yeast* **1995**, *11*, 301–310.
- (10) Patterson, J. H.; Waller, R. F.; Jeevarajah, D.; Billman-Jacobe, H.; McConville, M. J. *Biochem. J.* **2003**, *372*, 77–86.
- (11) Garami, A.; Ilg, T. J. *J. Biol. Chem.* **2001**, *276*, 6566–6575.
- (12) Shinabarger, D.; Berry, A.; May, T. B.; Rothmel, R.; Fialho, A.; Chakrabarty, A. M. *J. Biol. Chem.* **1991**, *266*, 2080–2088.
- (13) Wills, E. A.; Roberts, I. S.; Del Poeta, M.; Rivera, J.; Casadevall, A.; Cox, G. M.; Perfect, J. R. *Mol. Microbiol.* **2001**, *40*, 610–620.
- (14) Proudfoot, A. E. I.; Turcatti, G.; Wells, T. N. C.; Payton, M. A.; Smith, D. J. *Eur. J. Biochem.* **1994**, *219*, 415–423.
- (15) Proudfoot, A. E. I.; Payton, M. A.; Wells, T. N. C. *J. Protein Chem.* **1994**, *13*, 619–627.
- (16) Roux, C.; Lee, J. H.; Jeffery, C. J.; Salmon, L. *Biochemistry* **2004**, *43*, 2926–2934.
- (17) Roux, C.; Gresh, N.; Perera, L. E.; Piquemal, J.-P.; Salmon, L. *J. Comput. Chem.* **2007**, *28*, 938–957.
- (18) Roux, C.; Bhatt, F.; Foret, J.; de Courcy, B.; Gresh, N.; Piquemal, J.-P.; Jeffery, C. J.; Salmon, L. *Proteins* **2011**, *79*, 203–220.

- (19) Foret, J.; de Courcy, B.; Gresh, N.; Piquemal, J.-P.; Salmon, L. *Bioorg. Med. Chem.* **2009**, *17*, 7100–7107.
- (20) Gracy, R. W.; Noltman, E. A. *J. Biol. Chem.* **1968**, *243*, 5410–5419.
- (21) Langlet, J.; Claverie, P.; Caillet, J.; Pullman, A. *J. Phys. Chem.* **1988**, *92*, 1617–1631.
- (22) de Courcy, B.; Piquemal, J.-P.; Garbay, C.; Gresh, N. *J. Am. Chem. Soc.* **2010**, *132*, 3312–3320.
- (23) Gresh, N.; Claverie, P.; Pullman, A. *Theoret. Chim. Acta* **1984**, *66*, 1–20.
- (24) Gresh, N.; Pullman, A.; Claverie, P. *Theoret. Chim. Acta* **1985**, *67*, 11–32.
- (25) Gresh, N.; Cisneros, G. A.; Darden, T. A.; Piquemal, J.-P. *J. Chem. Theory Comput.* **2007**, *3*, 1960–1986.
- (26) Gresh, N. *J. Comput. Chem.* **1995**, *16*, 856–882.
- (27) Piquemal, J.-P.; Gresh, N.; Giessner-Prettre, C. *J. Phys. Chem. A* **2003**, *107*, 10353–10359.
- (28) Gresh, N.; Piquemal, J.-P.; Krauss, M. *J. Comput. Chem.* **2005**, *26*, 1113–1130.
- (29) Evangelakis, G. A.; Rizos, J. P.; Lagaris, I. E.; Demetropoulos, I. N. *Comput. Phys. Commun.* **1987**, *46*, 401–415.
- (30) Perdew, J. P.; Burke, K.; Ernzerhof, M. *Phys. Rev. Lett.* **1996**, *77*, 3865.
- (31) Perdew, J. P.; Burke, K.; Ernzerhof, M. *Phys. Rev. Lett.* **1997**, *78*, 1396.
- (32) Stevens, W. J.; Basch, H.; Krauss, M. *J. Chem. Phys.* **1984**, *81*, 6026–6033.
- (33) Dunning, T. H. *J. Chem. Phys.* **1989**, *90*, 1007.
- (34) Cammi, R.; Hofmann, H. J.; Tomasi, J. *Theoret. Chim. Acta* **1989**, *76*, 297–313.
- (35) Frisch, M. J.; Trucks, G. W.; Schlegel, H. B.; Scuseria, G. E.; Robb, M. A.; Cheeseman, J. R.; Scalmani, G.; Barone, V.; Mennucci, B.; Petersson, G. A.; Nakatsuji, H.; Caricato, M.; Li, X.; Hratchian, H. P.; Izmaylov, A. F.; Bloino, J.; Zheng, G.; Sonnenberg, J. L.; Hada, M.; Ehara, M.; Toyota, K.; Fukuda, R.; Hasegawa, J.; Ishida, M.; Nakajima, T.; Honda, Y.; Kitao, O.; Nakai, H.; Vreven, T.; Montgomery Jr., J. A.; Peralta, J. E.; Ogliaro, F.; Bearpark, M.; Heyd, J. J.; Brothers, E.; Kudin, K. N.; Staroverov, V. N.; Kobayashi, R.; Normand, J.; Raghavachari, K.; Rendell, A.; Burant, J. C.; Iyengar, S. S.; Tomasi, J.; Cossi, M.; Rega, N.; Millam, N. J.; Klene, M.; Knox, J. E.; Cross, J. B.; Bakken, V.; Adamo, C.; Jaramillo, J.; Gomperts, R.; Stratmann, R. E.; Yazyev, O.; Austin, A. J.; Cammi, R.; Pomelli, C.; Ochterski, J. W.; Martin, R. L.; Morokuma, K.; Zakrzewski, V. G.; Voth, G. A.; Salvador, P.; Dannenberg, J. J.; Dapprich, S.; Daniels, A. D.; Farkas, Ö.; Foresman, J. B.; Ortiz, J. V.; Cioslowski, J.; Fox, D. J. *Gaussian 09*, Revision A.1; Gaussian Inc.: Wallingford, CT.
- (36) Lambert, F.; Policar, C.; Durot, S.; Cesario, M.; Yuwei, L.; Korri-Youssoufi, H.; Keita, B.; Nadjo, L. *Inorg. Chem.* **2004**, *43*, 4178–4188.
- (37) Cleasby, A.; Wonacott, A.; Skarzynski, T.; Hubbard, R. E.; Davies, G. J.; Proudfoot, A. E. I.; Bernard, A. R.; Payton, M. A.; Wells, T. N. C. *Nat. Struct. Biol.* **1996**, *3*, 470–479.
- (38) Antony, J.; Piquemal, J.-P.; Gresh, N. *J. Comput. Chem.* **2005**, *26*, 1131–1147.
- (39) Gresh, N.; Audiffren, N.; Piquemal, J.-P.; de Ruyck, J.; Ledecq, M.; Wouters, J. *J. Phys. Chem. B* **2010**, *114*, 4884–4895.
- (40) Claverie, P.; Daudey, J. P.; Langlet, J.; Pullman, B.; Piazzola, D.; Huron, M. *J. Phys. Chem.* **1978**, *82*, 405–418.
- (41) Pullman, B.; Pullman, A.; Berthod, H.; Gresh, N. *Theoret. Chim. Acta* **1975**, *40*, 93–111.
- (42) *Insight II*; Accelrys Software Inc.: San Diego, CA.
- (43) Jiao, D.; Golubkov, P. A.; Darden, T. A.; Ren, P. *Proc. Natl. Acad. Sci. U.S.A.* **2008**, *105*, 6290–6295.
- (44) Jiao, D.; Zhang, J.; Duke, R. E.; Li, G.; Schnieders, M. J.; Ren, P. *J. Comput. Chem.* **2009**, *30*, 1701–1711.
- (45) Gresh, N. *J. Phys. Chem.* **1997**, *101*, 8680–8694.
- (46) Leach, A. R.; Shoichet, B. K.; Peishoff, C. E. *J. Med. Chem.* **2006**, *49*, 5851–5855.
- (47) Warren, G. L.; Andrews, C. W.; Capelli, A.-M.; Clarke, B.; LaLonde, J.; Lambert, M. H.; Lindvall, M.; Nevins, N.; Semus, S. F.; Senger, S.; Tedesco, G.; Wall, I. D.; Woolven, J. M.; Peishoff, C. E.; Head, M. S. *J. Med. Chem.* **2006**, *49*, 5912–5931.
- (48) Moitessier, N.; Englebienne, P.; Lee, D.; Lawandi, J.; Corbeil, C. R. *Br. J. Pharmacol.* **2009**, *153*, S7–S26.
- (49) Michel, J.; Foloppe, N.; Essex, J. W. *Mol. Inf.* **2010**, *29*, 570–578.
- (50) Chen, W.; Gilson, M. K.; Webb, S. P.; Potter, M. J. *J. Chem. Theory Comput.* **2010**, *6*, 3540–3557.
- (51) Wong, S.; Amaro, R. E.; McCammon, J. A. *J. Chem. Theory Comput.* **2009**, *5*, 422–429.
- (52) Abel, R.; Young, T.; Farid, R.; Berne, B. J.; Friesner, R. A. *J. Am. Chem. Soc.* **2008**, *130*, 2817–2831.
- (53) Luccarelli, J.; Michel, J.; Tirado-Rives, J.; Jorgensen, W. L. *J. Chem. Theory Comput.* **2010**, *6*, 3850–3856.
- (54) Michel, J.; Tirado-Rives, J.; Jorgensen, W. L. *J. Am. Chem. Soc.* **2009**, *131*, 15403–15411.
- (55) Park, M.-S.; Gao, C.; Stern, H. A. *Proteins* **2011**, *79*, 304–314.
- (56) Chang, C.-en A.; Chen, W.; Gilson, M. K. *Proc. Natl. Acad. Sci. U.S.A.* **2007**, *104*, 1534–1539.
- (57) Levy, R. M.; Karplus, M.; Kushick, J.; Perahia, D. *Macromolecules* **1984**, *17*, 1370–1374.
- (58) Karplus, M.; Kushick, J. N. *Macromolecules* **1981**, *14*, 325–332.
- (59) Thompson, J. D.; Higgins, D. G.; Gibson, T. J. *Nucleic Acids Res.* **1994**, *22*, 4673–4680.
- (60) Combet, C.; Blanchet, C.; Geourjon, C.; Deléage, G. *Trends Biochem. Sci.* **2000**, *25*, 147–150.
- (61) Gouet, P.; Robert, X.; Courcelle, E. *Nucleic Acids Res.* **2003**, *31*, 3320–3323.
- (62) DeLano, W. L. *The PyMOL molecular graphics system*; DeLano Scientific: San Carlos, CA, 2002.